

1 *Azadinium caudatum* var. *margalefii*, a poorly known member of the toxigenic genus

2 *Azadinium* (Dinophyceae)

3
4
5 URBAN TILLMANN*, BERND KROCK, BETTINA B. TAYLOR

6
7 *Alfred Wegener Institute for Polar and Marine Research, Bremerhaven, Germany*

8
9
10
11 Running title: *Azadinium caudatum* var. *margalefii*

12
13
14 *Corresponding author: Urban Tillmann, Alfred Wegener Institute for Polar and Marine

15 Research, Am Handelshafen 12, D-27570 Bremerhaven, Germany

16 Email address: Urban.Tillmann@awi.de

17 Phone +49 471 4831 1470; Fax +49 471 4831 1425

1 **Abstract**

2 *Azadinium caudatum* is a poorly known planktonic dinoflagellate, which mainly attracts
3 attention due to the occurrence of many toxigenic species in the genus *Azadinium*. The
4 availability of two Scottish isolates of *A. caudatum* var. *margalefii* allowed for the first time a
5 detailed analysis of biological and physiological traits of the species, specifically on the
6 potential presence of azaspiracid toxins (AZAs). With a mean overall swimming speed of 85
7 $\mu\text{m s}^{-1}$ and regularly interspersed high speed jumps, *A. caudatum* var. *margalefii* exhibited a
8 similar swimming behaviour to other species of the genus. Cells had a single, large, highly
9 reticulated chloroplast with a typical pigment composition for peridinin-containing
10 dinoflagellates. No pyrenoids were visible under light microscopy. A round to ovoid nucleus
11 was centrally located. Cell division was by desmoschisis, i.e. the parent theca was shared by
12 the daughter cells. Growth rate μ ranged from 0.07 to 0.32 d^{-1} and was reduced at lower
13 temperatures. With growth rate becoming light saturated at intensities of about 40 $\mu\text{E m}^{-2} \text{s}^{-1}$
14 and a half-saturation light intensity of about 13 $\mu\text{E m}^{-2} \text{s}^{-1}$, *A. caudatum* var. *margalefii*
15 appears to be relatively low light adapted. Neither strain produced any known AZAs in
16 measureable amounts.

17

18 Key words: *Azadinium caudatum*, azaspiracids, growth rate, morphology

19

1 **Introduction**

2

3 *Azadinium* is a dinophycean genus of planktonic algae mostly recognized due to its capability
4 to produce azaspiracids (AZAs), a recently discovered group of lipophilic phycotoxins
5 causing human intoxication via mussel consumption. After a first poisoning incident in the
6 Netherlands in 1995, azaspiracid toxins (AZAs) were isolated and chemically characterized
7 from Irish shellfish (Satake et al. 1998; Ofuji et al. 1999). Since then, AZA contamination of
8 mussels has been a recurrent and serious problem mainly in Ireland (Salas et al. 2011), but
9 AZAs have also been detected in samples from Europe, Morocco, Chile, China, and Japan
10 (Braña Magdalena et al. 2003; Taleb et al. 2006; Amzil et al. 2008; Ueoka et al. 2009; Alvarez
11 et al. 2010; Furey et al. 2010; Yao et al. 2010). The biogenic source of the toxins remained
12 elusive until the isolation and identification of a small new dinoflagellate species *Azadinium*
13 *spinosum* Elbrächter & Tillmann as a primary producer of AZA1 and AZA2 (Krock et al.
14 2009; Tillmann et al. 2009). Since then, the knowledge of the diversity of the genus has
15 increased rapidly and seven species are currently known. These comprise six newly described
16 species, *A. spinosum* (Elbrächter & Tillmann), *A. obesum* Tillmann & Elbrächter (Tillmann et
17 al. 2010), *A. poporum* Tillmann & Elbrächter (Tillmann et al. 2011), *A. polongum* Tillmann
18 (Tillmann et al. 2012b), *A. dexteroporum* Percopo & Zingone (Percopo et al. 2013), and *A.*
19 *dalianense* Luo, Gu & Tillmann (Luo et al. 2013). and the species *Azadinium caudatum*
20 (Halldal) Nézan & Chomérat, which was transferred to the genus (Nézan et al. 2012). Among
21 species of the family Amphidomataceae, to which the *Azadinium* species belong, production
22 of AZA toxins occurs in some, but not in all species; *A. spinosum*, *A. poporum* and the closely
23 related *Amphidoma languida* Tillmann, Salas & Elbrächter (Tillmann et al. 2012a) have been
24 shown to produce AZAs (Krock et al. 2012), whereas other species (*A. obesum*, *A. polongum*)
25 have been described as non-toxigenic (Krock et al. 2012; Tillmann et al. 2012b). For *A.*
26 *dexteroporum*, production of AZAs has been claimed (Percopo et al. 2013) but their presence

1 needs to be confirmed by LC-MS. Finally, for *A. caudatum*, there is no detailed analysis on
2 the presence of AZAs yet. This species was first described in 1953 by Halldal as *Amphidoma*
3 *caudata* off the Norwegian coast (Halldal 1953), and has been reported since from a
4 Portuguese lagoon (Silva 1968), around the British Isles, off the west coast of Ireland (Dodge
5 1982; Dodge & Saunders 1985), and, most recently, along the French Atlantic coast (Nézan et
6 al. 2012). The species is also present in the Mediterranean and has been reported from the
7 Ligurian Sea (Rampi 1969, as *Oxytoxum margalefi* and *Oxytoxum tonollii*), from the Spanish
8 coast (Margalef et al. 1954, as *Oxytoxum* sp., Delgado and Fortuño 1991, Margalef 1995),
9 from Adriatic Sea coasts (Viličić et al. 1995, Totti et al. 2000), and from the Gulf of Naples
10 (cited in Percopo et al. 2013). The first plate details provided by Dodge & Saunders (1985)
11 indicated that *Amphidoma caudata* had the same basic plate pattern as *Azadinium*. It was thus
12 concluded by Tillmann et al. (2011) that, notwithstanding some differences that remained to
13 be elucidated, *Amphidoma caudata* might be transferred to the genus *Azadinium*, pending
14 further morphological and phylogenetic studies. Subsequently, a study using field samples and
15 cultures of “*Amphidoma caudata*” used morphological and molecular data to clarify the
16 systematic situation and transferred the species to the genus *Azadinium* as *Azadinium*
17 *caudatum* (Nézan et al. 2012). Both sequence and morphometric data clearly showed that the
18 species occurred with two distinct varieties, var. *caudatum* and var. *margalefii*, which are
19 easily distinguished by the different shape of the antapical projection (Nézan et al. 2012).
20 On the basis of cultured strains of *A. caudatum* var. *margalefii* we are now adding more
21 detailed information to the species, most importantly including a detailed analysis of the
22 potential presence of AZAs. Furthermore, we performed additional light microscopy
23 observations on the morphology and swimming pattern, analysed the pigment profile,
24 elucidated one, yet missing detail on plate overlap pattern, described the mode of cell division
25 and collected quantitative data on growth performance for this little known dinoflagellate
26 species.

1
2
3
4
5
6
7
8
9
10
11
12
13
14
15
16
17
18
19
20
21
22
23
24
25
26

Material & Methods

Isolation and culturing

Two strains of *Azadinium caudatum* var. *margalefii* designated as AC1 and AC2 were isolated from a vertical net tow (0-20 m, 20 μm mesh size) taken in Scottish coastal waters at 58° 38.03' N, 3° 36.14' W during a cruise on FS “Heincke” in May 2011. Single cells were isolated using a capillary in multiwell plates and grown in K medium (Keller et al. 1987) prepared from filtered North Sea water. Established cultures were routinely grown in 65 ml plastic culture flasks at 15° C and 30 $\mu\text{E m}^{-1} \text{s}^{-1}$ at a light/dark cycle of 18:6 h. Cell size, plate pattern, and sequence data of both strains have been presented before (Nezan et al. 2012).

Light microscopy (LM)

Observation of cells was carried out with a stereomicroscope (Olympus SZH-ILLD) and with an inverted compound microscope (Axiovert 200 M, Zeiss, Germany) equipped with epifluorescence and differential interference contrast optics. The swimming pattern of cells was recorded with a video CCD camera (Sony DSP 3-CCD). For quantitative analysis of swimming speed, a culture growing at 20° C and 50 $\mu\text{E m}^{-2} \text{s}^{-1}$ was placed into an observation chamber (5 ml) over an inverted microscope and allowed to acclimate for 30 min at room temperature. Cells were subsequently recorded at a magnification of 320 x at 25 frames per second. The swimming tracks of 30 randomly chosen cells were analysed by single frame playback for the maximum time period in which the cell was in the focal plane.

Light microscopic examination of the thecal plates was performed on formalin-fixed cells (1 % final concentration) stained with calcofluor white (Fritz & Triemer 1985). The shape and localisation of the nucleus was determined after staining of formalin-fixed cells with 4'-6-

1 diamidino-2-phenylindole (DAPI, 0.1 $\mu\text{g ml}^{-1}$ final concentration) for 10 min. Photographs
2 were taken with a digital camera (Axiocam MRc5, Zeiss, Germany) connected to the inverted
3 microscope.

4 5 *Scanning electron microscopy (SEM)*

6 For SEM examination, cells from growing cultures were fixed, prepared, and collected on 3
7 μm polycarbonate filters (Millipore), as described by Tillmann et al. (2011). Filters were
8 mounted on stubs, sputter-coated (Emscope SC500, Ashford, UK) with gold-palladium and
9 viewed under a scanning electron microscope (FEI Quanta FEG 200, Eindhoven,
10 Netherlands). SEM micrographs were presented on a black background using Adobe
11 Photoshop 6.0 (Adobe Systems, San Jose, CA, USA).

12 13 *Growth experiments*

14 Growth performance of *A. caudatum* var. *margalefii* strain AC1 was quantified as follows: all
15 experimental cultures were grown in 65 ml plastic culture flasks. Initially, a stock culture was
16 grown at 15° C and 50 $\mu\text{E m}^{-2} \text{s}^{-1}$. From this stock culture, dilutions of 100 cells ml^{-1} were
17 prepared and adapted to the respective temperature and light conditions of the final growth
18 experiment for two weeks. After determining cell density in each adaptation set-up, triplicate
19 flasks with an initial cell density of 50 cells ml^{-1} were filled and incubated at the respective
20 experimental conditions. To evaluate the effect of temperature, cultures were grown at 10, 15,
21 and 20° C at a light intensity of 100 $\mu\text{E m}^{-2} \text{s}^{-1}$ in temperature adjusted growth chambers. To
22 evaluate effects of light, cultures grown at 15° C were incubated at 10, 50, 100 and 250 $\mu\text{E m}^{-2}$
23 s^{-1} . Light was measured using a 4π quantum sensor (LI 1000, LI-COR, Lincoln USA). In
24 order to analyse a potential growth enhancement effect of soil extract, one triplicate set of
25 flasks incubated at 15°C and 100 $\mu\text{E m}^{-2} \text{s}^{-1}$ received K-medium spiked with 1ml l^{-1} of soil
26 extract. Each flask was sampled every second day by removing 2 ml (for the first 3

1 samplings) or 1 ml (subsequent samplings). Flasks were refilled using fresh medium avoiding
2 large air-bubbles; refilling was accounted for when calculating growth rate. Sub-samples were
3 fixed with Lugol's solution (2% final concentration) and counted under an inverted
4 microscope. Growth rate (μ , d^{-1}) was calculated for a defined period of exponential increase
5 by calculating the exponential regression coefficient for a plot of cell numbers versus time.
6 When stationary phase was reached, pH in each flask was measured using an EcoScan pH5
7 (Eutech Instruments, Nijkerk, The Netherlands) pH-meter. Growth at different photon flux
8 densities was fitted to a Michaelis Menten model ($\mu = (\mu_{max} * I)/(k_s + I)$; I = photon flux
9 density, k_s = half saturation constant) using Statistica (StatSoft Inc, Tulsa, USA).

10

11 *Pigment analysis*

12 For pigment analysis, both strains were grown in 270 ml plastic culture flasks at the regular
13 culture conditions (see above). At a cell density of 1440 (AC1) and 1920 (AC2) per ml, as
14 estimated by microscopic cell counts, 250 ml were gently filtered on to a glass-fibre filter (25
15 mm \varnothing , GF/C, Whatman, Kent, UK). For AC1 a second filter was prepared on a different
16 occasion by filtering 250 ml of a cell density of 776 ml^{-1} . Filters were immediately shock-
17 frozen in liquid nitrogen and stored at $-80^{\circ} C$. Pigment composition was analyzed by High
18 Performance Liquid Chromatography (HPLC) following a method described by Hoffmann et
19 al. (2006) adjusted to our instruments as detailed by Taylor et al. (2011).

20

21 *Chemical analysis of AZAs*

22 Experimental cultures for toxin analysis were grown in 270 ml plastic culture flasks as
23 described above. Cells were harvested at the late exponential/early stationary phase. Different
24 batches of cultures were harvested and combined by gravity filtration through a 10 μm nitex
25 mesh. Cells were resuspended from the mesh in 50 ml filtered seawater in a 50 ml Falcon
26 tube. After taking a 0.5 ml sub-sample for cell counting, the tube was centrifuged (Eppendorf

1 5810R, Hamburg, Germany) at 3220 x g for 10 min and the cell pellet was transferred to an
2 Eppendorf microtube, centrifuged (Eppendorf 5415, 16,000 x g, 5 min) and stored at -20° C.
3 In total, four pellets of strain AC1 with a total number of 2.87 x 10⁶ cells and two pellets of
4 strain AC2 (total number: 0.86 x 10⁶ cells) were collected. For analysis each pellet was
5 thawed and suspended in 500 µl acetone, and transferred into a FastPrep tube containing 0.9 g
6 of lysing matrix D (Thermo Savant, Illkirch, France). The samples were homogenized by
7 reciprocal shaking at maximum speed (6.5 m s⁻¹) in a Bio101 FastPrep instrument (Thermo
8 Savant, Illkirch, France) for 45 s. After homogenization, samples were centrifuged (Eppendorf
9 5415 R, Hamburg, Germany) at 16,100 x g at 4° C for 15 min. All supernatants of each strain
10 were combined in a pear shaped flask and taken to dryness in a rotary evaporator (Büchi,
11 Konstanz, Germany). The residues were taken up in 500 µl acetone transferred to a 0.45 µm
12 pore-size spin-filter (Millipore Ultrafree, Eschborn, Germany) and centrifuged at 800 x g for
13 30 s. The filtrate was transferred into an LC autosampler vial for LC-MS/MS analysis.

14

15 *Single reaction monitoring (SRM) measurements*

16 Water was deionized and purified (Milli-Q, Millipore, Eschborn, Germany) to 18 MΩ cm⁻¹ or
17 better quality. Formic acid (90%, p.a.), acetic acid (p.a.) and ammonium formate (p.a.) were
18 purchased from Merck (Darmstadt, Germany). The solvents, methanol and acetonitrile, were
19 HPLC grade (Merck, Darmstadt, Germany).

20 Mass spectral experiments were performed to survey for a wide array of AZAs. The analytical
21 system consisted of an ABI-SCIEX-4000 Q Trap, triple quadrupole mass spectrometer
22 equipped with a TurboSpray[®] interface coupled to an Agilent model 1100 LC. The LC
23 equipment included a solvent reservoir, in-line degasser (G1379A), binary pump (G1311A),
24 refrigerated autosampler (G1329A/G1330B), and temperature-controlled column oven
25 (G1316A).

26 Separation of AZAs (5 µl sample injection volume) was performed by reverse-phase

1 chromatography on a C8 phase. The analytical column (50 × 2 mm) was packed with 3 μm
2 Hypersil BDS 120 Å (Phenomenex, Aschaffenburg, Germany) and maintained at 20 °C. The
3 flow rate was 0.2 ml min⁻¹ and gradient elution was performed with two eluents, where eluent
4 A was water and eluent B was acetonitrile/water (95:5 v/v), both containing 2.0 mM
5 ammonium formate and 50 mM formic acid. Initial conditions were 8 min column
6 equilibration with 30 % B, followed by a linear gradient to 100 % B within 8 min and
7 isocratic elution for 10 min with 100 % B then returning to initial conditions within 3 min
8 (total run time: 29 min).

9 AZA profiles were determined in one period (0 – 18) min with curtain gas: 10 psi, CAD:
10 medium, ion spray voltage: 5500 V, temperature: ambient, nebulizer gas: 10 psi, auxiliary
11 gas: off, interface heater: on, declustering potential: 100 V, entrance potential: 10 V, exit
12 potential: 30 V). SRM experiments were carried out in positive ion mode by selecting the
13 transitions (precursor ion > fragment ion) listed in the supplementary material (Tab. S1).

14 Cellular detection limits were calculated from signal to noise (S/N) ratios of an external
15 standard solution of AZA1 (certified reference material (CRM) programme of the IMB-NRC,
16 Halifax, Canada) based on an instrumental S/N > 3.

17

18 *Precursor ion experiments*

19 Precursors of the fragments m/z 348 and m/z 362 were scanned in the positive ion mode from
20 m/z 400 to 950 under the following conditions: curtain gas: 10 psi, CAD: medium, ion spray
21 voltage: 5500 V, temperature: ambient, nebulizer gas: 10 psi, auxiliary gas: off, interface
22 heater: on, declustering potential: 100 V, entrance potential: 10 V, collision energy: 70 V, exit
23 potential: 12 V.

24

25

26 **Results**

1 *General morphology*

2 *Azadinium caudatum* was quite easy to characterise by light microscopy due to its relatively
3 large size (length: 25.9–36.9 μm , width 18.9–25.8 μm , n = 154, measurements of strain AC1
4 and AC2 taken from Nézan et al. 2012), its characteristic triangular shape and its clearly
5 visible antapical projection (Fig. 1 A-E). This projection consisted of a blunt and short horn
6 and a well-developed spine (Fig. 1 C). The large nucleus located in the centre of the cell was
7 typically round to ovoid (Fig. 1 F, G) with clearly visible single chromosomes. Prior to
8 nuclear division the nucleus became enlarged and more elongated (Fig. 1 H). With LM there
9 were no indications of the presence of pyrenoid(s) but cells occasionally contained a number
10 of large spherical bodies which could be stained brown using Lugol's solution (Fig. 1 I, J).
11 Fluorescence microscopy revealed the presence of a presumably single but complex, highly
12 lobed retiform chloroplast extending both into the epi- and hyposome (Fig. 1 K-O). The
13 ventral/sulcal area, however, was devoid of chloroplasts with the finger-like extensions of the
14 plastid ending in that area (Fig. 1 N, O).

15

16 *Swimming pattern*

17 Like all other species of *Azadinium*, *A. caudatum* var. *margalefii* exhibited a characteristic
18 swimming pattern, i.e. swimming at a generally slow speed interrupted by sudden jumps (Fig.
19 2, see also video S1 provided as Supplementary material). Swimming paths generally were
20 straight or slightly curved (e.g. path no 14). Overall mean swimming speed of the swimming
21 paths depicted in Fig. 2 and quantified in Tab. 1 was 85 $\mu\text{m s}^{-1}$. During slow speed movement,
22 speed was typically in the range of 50-60 $\mu\text{m s}^{-1}$ (e.g. path no 8, 14, 26) but cells occasionally
23 travelled longer distances at a higher speed of 80 – 140 $\mu\text{m s}^{-1}$ (e.g. path no 3, 7). High-speed
24 jumps were accelerated changes in direction at an angle $> 45^\circ$, which most often was close to
25 90° (e.g. track no 4,6,11,12,24,25,28,29), but sudden path deviations more close to 45° were
26 also observed (e.g. path no. 15,30). Short-duration maximum speed during these jumps has

1 been calculated as approx. $360 \mu\text{m s}^{-1}$.

2

3 *Plate overlap*

4 The whole plate overlap or imbrication pattern for *Azadinium caudatum* was reported in
5 Nézan et al. (2012). However, one interesting detail could not be resolved there and is
6 reported here using SEM (Fig. 3). In the ventral area, the anterior sulcal plate (Sa) was
7 overlapped by its left neighbouring cingular plate C1 but overlapped the right neighbouring
8 plate C6 (Fig. 3 B-D). Thus, for the midventral area plate C6 and not plate Sa was overlapped
9 by all adjacent plates.

10

11 *Division mode*

12 Dividing cells mainly increased the cell width (Fig. 4 A, M). Throughout the whole
13 cytokinetic process, cells of *Azadinium caudatum* kept their motility. Cell division was by
14 desmoschisis, i.e. the parent theca was shared by the daughter cells (Fig. 4 A-P). Thecal plates
15 were separated along a well defined oblique fission line separating an anterosinistral part from
16 a posterodextral part. The line of the border could already be defined by light microscopy of
17 calcofluor stained thecae (Fig. 4 C-L) and could additionally be depicted by SEM (Fig. 4 M-
18 P). Along this fission line, as schematized in Fig. 4 Q-R, the anterosinistral daughter cell
19 received the apical plates (including the APC), the epithelial intercalary plates, the first two
20 precingular plates, the anterior sulcal plate (Sa), and the first three postcingular plates. The
21 posterodextral daughter cell obtained both antapical plates together with the remaining
22 postcingular plates, the large posterior sulcal plate (Sp), and, from the epithelial plates, the
23 third and all following precingular plates. The distribution, if any, of other small sulcal plates
24 could not be resolved. For the cingular plates, the fission line separated plate C3 and C4. Even
25 in advanced stages of cell division, there were no indications of newly formed plate material
26 (Fig. 4 G, H) and freshly divided cells still seemed to lack the missing thecal parts (Fig. 4 I-L).

1 The course of the fission line is in agreement with the described plate overlap pattern of *A.*
2 *caudatum* in that there is a consistent overlap along the fission line of the epitheca. For the
3 hypotheca, however, there was one exception as the first antapical plate of *A. caudatum*
4 overlapped the first postcingular plate (see, Fig. 3 B), opposite to the notion that hypothecal
5 plates of the left daughter cell overlap plates of the right daughter cell.

6

7 **Growth rate**

8 Growth curves of *Azadinium caudatum* var *margalefii* strain AC1 are plotted in Fig. 5. For all
9 experimental conditions exponential growth started immediately without any obvious lag-
10 phase. Exponential growth persisted for 7 ($100 \mu\text{E m}^{-2} \text{s}^{-1}$, 20°C , Fig. 5 B)) to 27 days (100
11 $\mu\text{E m}^{-2} \text{s}^{-1}$, 10°C , Fig. 5 F), before a period of continuously decreasing growth rate preceded
12 the stationary phase. Maximum cell densities varied between 2400 (15°C , $40 \mu\text{E m}^{-2} \text{s}^{-1}$, Fig.
13 5 C) and 600 (10°C , $100 \mu\text{E m}^{-2} \text{s}^{-1}$, Fig. 5 F), but growth at the latter condition probably was
14 not at its end when the experiment was terminated after 40 days. At a fixed light intensity of
15 $100 \mu\text{E m}^{-2} \text{s}^{-1}$ exponential growth rate increased with temperature (Fig. 5, right panel), being
16 highest at 20°C ($\mu = 0.32 \pm 0.02 \text{ d}^{-1}$). At 15°C growth was slightly but significantly (t- test, p
17 < 0.05) lower and drastically dropped down to $0.07 \pm 0.005 \text{ d}^{-1}$ at 10°C (Fig. 5 H). At a fixed
18 temperature of 15°C growth increased with increasing irradiance from $0.15 \pm 0.01 \text{ d}^{-1}$ at 15
19 $\mu\text{E m}^{-2} \text{s}^{-1}$ to $0.27 \pm 0.01 \text{ d}^{-1}$ at $250 \mu\text{E m}^{-2} \text{s}^{-1}$ and was almost saturated at $40 \mu\text{E m}^{-2} \text{s}^{-1}$ (Fig. 5
20 G). Fitting the data to a Michaelis Menten formula (Fig. 5 G) revealed a maximum growth of
21 0.295 d^{-1} and a half saturation light intensity for growth of $13 \mu\text{E m}^{-2} \text{s}^{-1}$. The pH measured at
22 day 21 was low ranging from 8.18 to 8.30 (Fig. 5 A-F)). Growth rate and final cell yield for
23 cultures enriched with soil extract (data not shown) were not significantly different compared
24 to cultures grown with regular K-medium (t-test, $p > 0.05$).

25

26 *Pigment profile*

1 Figure 6 shows the typical chromatogram of the *Azadinium caudatum* var *margalefii* AC1
2 pigment analysis. Pigments were identified by co-chromatography of known pigment
3 standards, but some peaks could not be assigned to any standard available in our library. In
4 the *A. caudatum* var. *margalefii* AC1 strain, three unknown pigments were detected (x1, x2,
5 and x3). The chromatogram of the AC2 strain only differs from the AC1 strain by having one
6 additional unknown pigment at a retention time of 12.08 minutes, which was present in trace
7 amounts (unknown pigment x4, chromatogram not shown). Figure 7 show the absorption
8 spectra of all 4 unknown pigments. The pigment composition of the quantifiable pigments of
9 *A. caudatum* var. *margalefii* AC1 (not different for AC2 and thus not shown here) is listed in
10 Tab. 2. Besides the main photosynthetic pigment chlorophyll *a* which accounted for 42 % of
11 total pigment, peridinin with 38 % of total pigment was the most conspicuous pigment,
12 followed by chlorophyll *c*₁ + *c*₂ which accounted for 10 % of total pigment. Chlorophyll *c*₁ +
13 *c*₂ could not be separated with our method.

14

15 *Azaspiracids*

16 Using the selected reaction monitoring mode (SRM), no known AZAs could be detected in
17 either *Azadinium caudatum* var. *margalefii* strain. The detection limit on a cellular basis was
18 estimated as 0.06 fg cell⁻¹ for AC1 and 0.2 fg cell⁻¹ for AC2 (higher due to the lower biomass
19 of the sample). In addition, precursor ion experiments for detecting putative precursor masses
20 of the characteristic collision induced dissociation (CID)-fragments *m/z* 348 and *m/z* 362 of
21 AZAs did not give any further signals for neither AC1 nor AC2, indicating that neither strain
22 produced other unknown AZA variants in larger amounts. However, the precursor ion mode is
23 approximately a hundred times less sensitive than the SRM mode and strictly speaking does
24 not allow for exact quantitative measurement. Considering a conservatively determined
25 “detection limit” of 81 pg on the column, this represents a cellular detection limit of unknown
26 AZA variants of 3 fg (AC1) or 10 fg (AC2).

1

2

3 **Discussion**

4 For most of the approximately 2500 described species of dinoflagellates (Elbrächter 2003),
5 only some taxonomically relevant morphological features are known, but additional
6 information about morphology, physiology, behaviour, life cycle, or cellular compounds is
7 still scarce, mainly due to both the lack of live cell observations and/or availability of cultures.

8 This is especially true for the vast majority of “rare” species that do not attract attention as
9 bloom forming species do. *Azadinium caudatum* is a very good example of such a “rare”
10 species, which has been described in terms of morphology (Halldal 1953; Dodge & Saunders
11 1985), even in great detail (Nézan et al. 2012), but which has never been reported to occur in
12 higher densities and for which almost no biological and/or physiological details are known.

13 *Azadinium caudatum*, and this refers to both varieties var. *margalefii* and var. *caudatum*, is a
14 case where the characteristic shape in combination with size and the presence of a single and
15 prominent antapical spine unambiguously allows for a species designation based on just light
16 microscopy even of fixed samples. Nevertheless, knowledge on other cellular features like
17 chloroplast arrangement, shape and location of the nucleus and the potential presence of
18 pyrenoid(s) could further assist in species designation and allows comparing these features
19 with other members of the Amphidomataceae.

20

21 *Swimming pattern:*

22 With a relatively slow swimming speed interrupted by short, high speed “jumps“ in various
23 directions, *Azadinium caudatum* var. *margalefii* exhibits the same conspicuous swimming
24 behaviour described for other species of the Amphidomataceae (e.g. Tillmann et al. 2009;
25 Tillmann et al. 2012a). With an overall mean speed of $85 \mu\text{m s}^{-1}$, *A. caudatum* var. *margalefii*

1 is considerably slower than *A. poporum* ($400 \mu\text{m s}^{-1}$), the only species for which quantitative
2 data are available (Potvin et al. 2013). Generally, the swimming speed of *A. caudatum* var.
3 *margalefii* is at the low end of the range of swimming speeds reported for other
4 dinoflagellates (ca. $20 - 500 \mu\text{m sec}^{-1}$, Smayda 2002a); for chain forming species even higher
5 swimming velocities of $856 \mu\text{m s}^{-1}$ have been reported (Sohn et al. 2011). Species of the
6 Amphidomataceae generally seem to swim at a relatively slow speed. *Amphidoma languida* ,
7 although not explicitly quantified, seem to be particularly slow in its general movement
8 (Tillmann et al. 2012a) and might be even slower than *A. caudatum* var. *margalefii*, which is
9 reflected in its name (*languida* (lat.) = lazy, slow). Although all species of Amphidomataceae
10 may rarely travel larger distances at a higher speed, they usually exhibit interspersed jumps,
11 quite regularly when approaching other objects, e.g. when reaching the glass bottom of the
12 observation chamber. As quantified here for *A. caudatum* var. *margalefii*, the maximum speed
13 of these jumps can be about seven times higher than regular speed, but this maximum speed
14 of approx. $350 \mu\text{m s}^{-1}$ is still slow compared to jump velocities of ciliated protists which are in
15 the range of 2000 to $5000 \mu\text{m s}^{-1}$ (Jakobsen 2001). The change of direction related to these
16 jumps, quantified here as mostly close to 90° , is consistent with the idea that these jumps act
17 as an avoidance behaviour and probably represent a direct escape mechanism involved in
18 predator/prey interactions (Jakobsen 2001; Jakobsen 2002; Tillmann 2004).

19

20 *Chloroplast, pyrenoid, nucleus:*

21 A general survey of chloroplast morphology of dinoflagellates indicated that larger species
22 often possess numerous small and more globular plastids, whereas small species generally are
23 characterised by one or very few but large reticulate and parietally arranged chloroplasts
24 (Schnepf & Elbrächter 1999). *Azadinium caudatum* var. *margalefii*, like all other species of
25 Amphidomataceae, clearly is photosynthetic with a chloroplast of the latter type, i.e. they
26 possess a presumably single chloroplast which is parietally arranged and normally extends

1 into both the epi- and hyposome. The degree of reticulation of the chloroplast of *A. caudatum*
2 var. *margalefii* forming a filamentous network, however, seems to be considerably higher
3 compared to other species of *Azadinium*.

4 The presence/absence, location, number and types of pyrenoids have been regarded as useful
5 taxonomic characters at the genus level (Schnepf & Elbrächter 1999) and have in particular
6 been discussed as potential features visible in light microscopy to differentiate between
7 species of *Azadinium* (Tillmann et al. 2011). In particular, stalked pyrenoid(s) are visible
8 under the light microscope because of a distinct starch cup. *Azadinium caudatum* var.
9 *margalefii* clearly lacks this type of pyrenoid(s) visible under the light microscope and is thus
10 similar to *A. obesum* and *A. polongum* (no visible pyrenoids) (Tillmann et al. 2010; Tillmann
11 et al. 2012b), but different from *A. spinosum*, *A. dexteroporum* (one pyrenoid) (Tillmann et al.
12 2009; Percopo et al. 2013), and *A. poporum* and *A. dalianense* (several pyrenoids) (Tillmann
13 et al. 2011; Luo et al. 2013).

14 In many species of dinoflagellates the nucleus is large and conspicuous (Dodge 1963) and
15 thus nuclear shape and location is often included in species descriptions. As for all other
16 species of Amphidomataceae the nucleus of *A. caudatum* var. *margalefii* was generally round
17 to slightly ovoid and was positioned in a slightly posterior position in the cell centre.

18 Nevertheless, cells with an elongated nucleus have been observed, which most probably
19 reflects an advanced state in nuclear division. Such a distinct change in the shape of the
20 nucleus has also been noted as the first sign of nuclear division for many dinoflagellates
21 (Dodge 1963). For both *A. languida* and in more detail, for *A. spinosum*, a distinct elongation
22 of the round to elliptical nucleus in the course of nuclear division has been described
23 (Tillmann et al. 2012a; Tillmann & Elbrächter 2013).

24

25 *Imbrication:*

26 Ultrastructural details (plate pattern) have thoroughly been analysed previously (Nézan et al.

1 2012), showing that both varieties of *A. caudatum* have the typical Kofoidian plate pattern of
2 the genus *Azadinium*, but differ by the antapical spine and the position of the ventral pore.
3 Plate pattern analysis by Nézan et al. (2012) included an analysis of the plate overlap (or
4 imbrication pattern), which may give insights on functional aspects of ecdysis and/or on the
5 archeopyle type of cysts, and which may be a useful aid in determining plate homologies
6 (Netzel & Dürr 1984). It has been elucidated in details for *A. spinosum* (Tillmann &
7 Elbrächter 2010), *A. languida* (Tillmann et al. 2012a), *A. caudatum* (Nézan et al. 2012) and *A.*
8 *polongum* (Tillmann et al. 2012b). The pattern was consistent among the species, with an
9 uncommon but stable imbrication pattern of the most dorsal apical plate (3' in *Azadinium* or 4'
10 in *Amphidoma* is overlapped by all adjacent plates), which characterized these two genera and
11 might be helpful for a revision of the description of the family Amphidomataceae. Another
12 peculiarity of imbrication of *Azadinium* species was identified for the overlap of the central
13 ventral plate: in contrast to other dinophycean species (Netzel & Dürr 1984), the last cingular
14 plate C6 of *Azadinium* species and *A. languida* have been shown to be overlapped by all
15 adjacent plates, instead of the central sulcal plate Sa. This important feature had not been
16 resolved for *A. caudatum* in the imbrication analysis by Nézan et al. (2012) and is reported
17 here to be exactly the same for *A. caudatum* var. *margalefii*, indicating that this feature might
18 also be characteristic for these two genera and might be helpful for a revision of the
19 description of the family Amphidomataceae.

20

21 *Cell division:*

22 With few exceptions, the vegetative reproduction of dinoflagellates is by binary fission
23 (Elbrächter 2003). Thecate dinoflagellates can divide either by entirely shedding the parent
24 theca so that both sister cells have to rebuild a whole new theca (eleuteroschisis), or by
25 sharing the parent theca between the two daughter cells (desmoschisis; Pfister & Anderson
26 1987; Elbrächter 2003). The desmoschisis type of cell division of *A. caudatum* var. *margalefii*

1 was similar to the cell division described for *A. spinosum* (Tillmann & Elbrächter 2013) and
2 *A. languida* (Tillmann et al. 2012a) and exhibited exactly the same position of the fission line
3 as described for *A. spinosum*. Moreover, some features of desmoschisis, which have been
4 described for *A. spinosum* as peculiar and different from desmoschisis of Gonyaulacean
5 species (Tillmann & Elbrächter 2013), are also found for *A. caudatum* var. *margalefii*. This
6 refers particularly to the relation of fission line and plate overlap, which for
7 Amphidomataceae seem to be characterised by an analogy in the epitheca (all plates of the
8 anterosinistral part are overlapped by plates of the posterodextral part, see Fig. 4 Q), but
9 which show one deviation of that pattern for the hypotheca (Tillmann & Elbrächter 2013)
10 (Fig. 4 R). As in *A. languida* and *A. spinosum*, freshly divided cells of *A. caudatum* var.
11 *margalefii* seem not to have completed the formation of new rigid thecal plates. Such a
12 delayed thecal plate formation stands in contrast to catenate species of the genus
13 *Alexandrium*, where it appears that the new thecae are being formed as cytokinesis progresses
14 (Tomas 1974).

15

16 *Growth experiments:*

17 With a maximum growth rate of strains AC1 of 0.32 d^{-1} (corresponding to about 0.5 divisions
18 per day) at 20° C and $100 \mu\text{E m}^{-2} \text{ s}^{-1}$, *Azadinium caudatum* var. *margalefii* seems to be a
19 generally slow growing species compared to many other dinoflagellates which normally are
20 able to divide approximately once per day at optimal conditions (Banse 1982; Smayda 1997;
21 Smayda 2002b). The maximum growth is also slower compared to *A. spinosum*, the only
22 species of Amphidomataceae for which quantitative growth data are available (Jauffrais et al.
23 2013). Growth of *A. caudatum* var. *margalefii* was gradually affected by both temperature and
24 light in very much the same way as *A. spinosum* (Jauffrais et al. 2013). By testing just three
25 temperatures covering a relatively narrow range from 10° to 20° C , upper and lower
26 temperature limits for positive growth of *A. caudatum* var. *margalefii* AC1 are not yet

1 precisely defined. *A. caudatum* var. *margalefii* has been described from both the distinctly
2 warmer Mediterranean area (Rampi 1969) and the temperate French and Irish Atlantic coast
3 and around the British Isles (Dodge & Saunders 1985; Nézan et al. 2012). Occurrence of *A.*
4 *caudatum* var. *margalefii* in more northern areas is unknown; records of *A. caudatum* in
5 Northern Norwegian waters during winter (Halldal 1953) referred to the other variety var.
6 *caudatum* and thus might reflect different temperature requirements of var. *caudatum* and var.
7 *margalefii*.

8 *Azadinium caudatum* var. *margalefii* appears to be low light adapted, indicated by growth
9 rates of strain AC1 becoming light saturated at intensities of about $40 \mu\text{E m}^{-2} \text{s}^{-1}$ and a half-
10 saturation light intensity of about $13 \mu\text{E m}^{-2} \text{s}^{-1}$. For bloom forming dinoflagellates like
11 *Ceratium furca* (Ehrenberg) Claparède & Lachmann and *C. fusus* (Ehrenberg) Dujardin,
12 optimal growth was recorded at light intensities $> 200 \mu\text{E m}^{-2} \text{s}^{-1}$ characterizing those species
13 as well-adapted to high intensity light levels (Baek et al. 2008), as are other bloom forming
14 species of the genus *Alexandrium* (Fu et al. 2012) or *Cochlodinium* (Kim et al. 2004).

15 However, low light adaptation is not an exclusion criterion for bloom formation as other
16 bloom forming species like *Karenia brevis* (C.C. Davis) G. Hansen & Moestrup (Magana &
17 Villareal 2006) are known to be low light adapted as well. For *A. caudatum* var. *margalefii*
18 AC1, there was no photoinhibition of growth at the highest light intensity tested ($250 \mu\text{E m}^{-2}$
19 s^{-1}) indicating that this species, although adapted to low light, can cope with higher light in
20 subsurface water. However, growth response at high light levels, typical for peak subsurface
21 summer values of up to $2000 \mu\text{E m}^{-2} \text{s}^{-2}$ (Kirk 1994) still needs to be tested. The light
22 response of *A. caudatum* var. *margalefii* AC1 was similar to that of *A. spinosum* giving no
23 signs of photoinhibition at higher light levels (tested up to $400 \mu\text{mol m}^{-2} \text{s}^{-1}$) and growth was
24 almost saturated down to the lowest light level tested ($50 \mu\text{mol m}^{-2} \text{s}^{-1}$) (Jauffrais et al. 2013).

25 In our culture experiments, the final cell yield of strain AC1 at the stationary phase was
26 conspicuously low ($< 2400 \text{ cells ml}^{-1}$). It is not clear which factor was crucial for growth

1 cessation in these batch cultures: concentration of macronutrients (nitrate and phosphate) in
2 the medium applied here are excessive and should allow for a much higher biomass, as they
3 normally do for other species like *Alexandrium tamarense* (Lebour) Balech (e.g. Zhu &
4 Tillmann 2012). Adding soil extract did not increase growth rate and yield, making a lack of
5 trace elements unlikely. Prolonged growth in un-bubbled cultures might lead to carbon
6 limitation. In addition, high pH has been shown to strongly affect dinoflagellate growth of
7 both photosynthetic and heterotrophic species (Hansen 2002; Pedersen & Hansen 2003).
8 Culture growth experiments (Hansen et al. 2007) and physiological studies of inorganic
9 carbon acquisition in red tide dinoflagellates (Rost et al. 2006) both suggest that marine
10 dinoflagellates may not be carbon-limited even at high pH, thus direct effects of high pH
11 might be responsible for growth cessation (Hansen et al. 2007). The pH measured during the
12 stationary phase of *A. caudatum* var. *margalefii* was quite low (around 8.3), but still in the
13 range of the lowest pH tolerance limits reported in the literature; for species of *Ceratium* or
14 the dictyochophyte *Dictyocha speculum* Ehrenberg, pH values affecting exponential growth
15 of 8.24-8.30 have been reported (Schmidt & Hansen 2001), although upper pH limit for
16 growth of *Ceratium* spp. later was reported to be in the range of 8.7 – 9.1 (Soederberg &
17 Hansen 2007). Further detailed experiments are needed to clarify whether *A. caudatum* has an
18 extraordinary low pH tolerance and/or is an extraordinarily poor competitor for carbon, or if
19 other exceptional trace compounds not included in the soil extract might have been yield-
20 limiting. In any case, low final cell yield in our batch culture experiment would support the
21 notion that *A. caudatum* is generally found in low abundances in field samples (Nézan et al.
22 2012).

23

24 *Pigments:*

25 Both available strains of *Azadinium caudatum* var. *margalefii* showed a typical pigment
26 composition for peridinin-containing dinoflagellates with chlorophyll $c_{1/2}$ as the main

1 accessory chlorophyll and peridinin as the main carotenoid. Diadinoxanthin, dinoxanthin,
2 diatoxanthin and β -carotene are also typical for peridinin-containing dinoflagellates and have
3 been reported for other closely related species (Tillmann et al. 2009; Tillmann et al. 2010;
4 Tillmann et al. 2012a; Zapata et al. 2012). Violaxanthin has not been reported for *Azadinium*-
5 species before and was only detected in trace amounts here. Prasinolaxanthin, which was
6 reported in low amounts for other *Azadinium* species (Tillmann et al. 2009; Tillmann et al.
7 2010), could not be detected in the present analysis.

8 The unknown pigments are probably all carotenoids. Unknown pigment x1 shows an
9 absorption spectrum similar to peridinin with a single maximum at 465 nm and has previously
10 been reported from peridinin-containing dinoflagellates by Zapata et al. (2012). It elutes
11 approx. 1.5 minutes later than peridinin. Unknown pigments x2 and x3 have absorption
12 spectra similar to gyroxanthin-diester, what has previously been reported from dinoflagellates
13 such as *K. brevis* (Bjørnland et al. 2003). Unknown pigment x2 elutes approximately 5
14 minutes earlier and is thus more polar than unknown pigment x3. A gyroxanthin diester-like
15 pigment, probably similar to our unknown pigment x3, has been reported by Zapata et al.
16 (2012) in dinoflagellate species containing fucoxanthin as their major carotenoid. The
17 absorption spectrum of unknown pigment x4, which was only detected in traces in the AC2
18 strain, resembles the carotenoid lycopene.

19

20 *Toxins:*

21 The presence of azaspiracids in shellfish has been a recurring problem in Ireland since 2005,
22 with levels above the regulatory limit of 0.16 mg AZAs per kg mussel observed mainly in
23 blue mussels. First feeding studies clearly showed a direct link between *Azadinium spinosum*
24 and AZA contamination of mussels. However, concentrations of AZAs found in mussels
25 during laboratory exposures (Salas et al. 2011; Jauffrais et al. 2012) were still ca. 10-fold
26 lower than the maximum concentrations encountered in the field, so we still have to consider

1 alternative AZA sources, like the presence of other yet unidentified cryptic AZA-producing
2 species. In this respect, *A. caudatum* has been an interesting candidate, as it is a close relative
3 of *A. spinosum*, is known to occur in Irish waters (Dodge & Saunders 1985), and is relatively
4 large compared to *A. spinosum* (which implies a potentially larger cell toxin quota). However,
5 we failed to detect known AZAs and other compounds producing AZA-characteristic MS-
6 fragments in both strains of *A. caudatum* var. *margalefii*, but of course we cannot exclude the
7 presence of other related molecules, specifically as a high variability in AZA toxin profile has
8 been described for at least one species of *Azadinium*, *A. poporum* (Krock et al. 2012; Gu et al.
9 2013). Most notably, among a total of ten strains of *A. poporum* analyzed so far, one strain
10 was found without any detectable AZAs (Gu et al. 2013). With just two strains of *A. caudatum*
11 var. *margalefii* available and examined so far, clearly more strains, including strains of the
12 variety *A. caudatum* var. *caudatum*, need to be established and analyzed in the future to
13 evaluate if the absence of AZAs is a constant trait of *A. caudatum*.

14

1 **References**

- 2 Alvarez G, Uribe E, Avalos P, Marino C, Blanco J. 2010. First identification of azaspiracid
3 and spirolides in *Mesodesma donacium* and *Mulinia edulis* from Northern Chile.
4 *Toxicon* 55:638-41.
- 5 Amzil Z, Sibat M, Royer F, Savar V. 2008. First report on azaspiracid and yessotoxin groups
6 detection in French shellfish. *Toxicon* 52:39-48.
- 7 Baek SH, Shimode S, Kikuchi T. 2008. Growth of dinoflagellates, *Ceratium furca* and
8 *Ceratium fusus* in Sagami Bay, Japan: The role of temperature, light intensity and
9 photoperiod. *Harmful Algae* 7:163-73.
- 10 Banse K. 1982. Cell volumes, maximal growth rates of unicellular algae and ciliates, and the
11 role of ciliates in the marine pelagial. *Limnology and Oceanography* 27:1059-71.
- 12 Bjørnland T, Haxo FT, Liaaen-Jensen S. 2003. Carotenoids of the Florida red tide
13 dinoflagellate *Karenia brevis*. *Biochemical Systematics and Ecology*. 31:1147–62.
- 14 Braña Magdalena A, Lehane M, Krys S, Fernandez ML, Furey A, James KJ. 2003. The first
15 identification of azaspiracids in shellfish from France and Spain. *Toxicon* 42:105-8.
- 16 Delgado, M. & Fortuño, J. M. 1991. Atlas de fitoplancton del Mar Mediterráneo. *Sci. Mar.* 55
17 (Suppl. 1):1–133.
- 18 Dodge JD. 1963. The nucleus and nuclear division in the Dinophyceae. *Archiv für*
19 *Protistenkunde* 106:442-52.
- 20 Dodge JD, 1982. *The Dinoflagellates of the British Isles*. London: Her Majesty's Stationery
21 Office. 303 pages.
- 22 Dodge JD, Saunders RD. 1985. An SEM study of *Amphidoma nucula* (Dinophyceae) and
23 description of the thecal plates in *A. caudata*. *Archiv für Protistenkunde* 129:89-99.
- 24 Elbrächter M. 2003. Dinophyte reproduction: progress and conflicts. *Journal of Phycology*
25 39:629-32.
- 26 Fritz L, Triemer RE. 1985. A rapid simple technique utilizing Calcofluor white M2R for the
27 visualization of dinoflagellate thecal plates. *Journal of Phycology* 21:662-4.
- 28 Fu FX, Tatters AO, Hutchins DA. 2012. Global change and the future of harmful algal blooms
29 in the ocean. *Marine Ecology Progress Series* 470:207-33.
- 30 Furey A, O'Doherty S, O'Callaghan K, Lehane M, James KJ. 2010. Azaspiracid poisoning
31 (AZP) toxins in shellfish: Toxicological and health considerations. *Toxicon* 56:173-90.
- 32 Gu H, Luo Z, Krock B, Witt M, Tillmann U. 2013. Morphology, phylogeny and azaspiracid
33 profile of *Azadinium poporum* (Dinophyceae) from the China Sea. *Harmful Algae* 21-
34 22:64-75.

- 1 Halldal P. 1953. Phytoplankton investigations from Weather Ship M in the Norwegian Sea,
2 1948-49. Hvalrådets Skrifter 38:1-91.
- 3 Hansen PJ. 2002. Effect of high pH on the growth and survival of marine phytoplankton:
4 implications for species succession. *Aquatic Microbial Ecology* 28:279-88.
- 5 Hansen PJ, Lundholm N, Rost B. 2007. Growth limitation in marine red-tide dinoflagellates:
6 effects of pH versus inorganic carbon availability. *Marine Ecology Progress Series*
7 334:63-71.
- 8 Hoffmann L, Peeken JI, Lochte K, Assmy P, Veldhuis M. 2006. Different reactions of
9 Southern Ocean phytoplankton size classes to iron fertilization. *Limnology and*
10 *Oceanography* 51:1217-29.
- 11 Jakobsen HH. 2001. Escape response of planktonic protists to fluid mechanical signals. *Marine*
12 *Ecology Progress Series* 214:67-78.
- 13 Jakobsen HH. 2002. Escape of protists in predator-generated feeding currents. *Aquatic*
14 *Microbial Ecology* 26:271-81.
- 15 Jauffrais T, Marcaillou C, Herrenknecht C, Truquet P, Séchet V, Nicolau E, et al. 2012.
16 Azaspiracid accumulation, detoxification and biotransformation in blue mussels
17 experimentally fed *Azadinium spinosum* (Dinophyceae) *Toxicon* 60:582-95.
- 18 Jauffrais T, Séchet V, Herrenknecht C, Truquet P, Veronique S, Tillmann U, et al. 2013. Effect
19 of environmental and nutritional factors on growth and azaspiracid production of the
20 dinoflagellate *Azadinium spinosum* *Harmful Algae* 27:138-48.
- 21 Keller MD, Selvin RC, Claus W, Guillard RRL. 1987. Media for the culture of oceanic
22 ultraphytoplankton. *Journal of Phycology* 23:633-8.
- 23 Kim DI, Matsuyama Y, Nagasoe S, Yamaguchi M, Yoon YH, Oshima Y, et al. 2004. Effects of
24 temperature, salinity and irradiance on the growth of the harmful red tide dinoflagellate
25 *Cochlodinium polykrikoides* Margalef (Dinophyceae). *Journal of Plankton Research*
26 26:61-6.
- 27 Kirk JTO, 1994. *Light & Photosynthesis in Aquatic Ecosystems*. Cambridge: Cambridge
28 University Press. 509 pages.
- 29 Krock B, Tillmann U, John U, Cembella AD. 2009. Characterization of azaspiracids in
30 plankton size-fractions and isolation of an azaspiracid-producing dinoflagellate from
31 the North Sea. *Harmful Algae* 8:254-63.
- 32 Krock B, Tillmann U, Voß D, Koch BP, Salas R, Witt M, et al. 2012. New azaspiracids in
33 Amphidomataceae (Dinophyceae): proposed structures. *Toxicon* 60:830-9.

- 1 Luo Z, Gu H, Krock B, Tillmann U. 2013. *Azadinium dalianense*, a new dinoflagellate from
2 the Yellow Sea, China. *Phycologia* 52: 625-636
- 3 Magana HA, Villareal TA. 2006. The effect of environmental factors on the growth rate of
4 *Karenia brevis* (Davis) G. Hansen and Moestrup. *Harmful Algae* 5:192-8.
- 5 Margalef R, Herrera J, Rodriguez-Roda J, Larrañeta M. 1954. Plancton recogido por los
6 laboratorios costeros, VIII. Fitoplancton de las costas de Castellón durante el año
7 1952. *Publicaciones del Instituto de Biología Aplicada* 17:87-100.
- 8 Margalef, R. 1995. Fitoplancton del NW del Mediterraneo (Mar Catalan) en junio de 1993, y
9 factores que condicionan su producción y distribución. *Memorias de la Real*
10 *Academia de Ciencias y Artes de Barcelona* 60:1-56.
- 11 Netzel H, Dürr G. 1984. Dinoflagellate Cell Cortex. In: Spector DL, editor. *Dinoflagellates*.
12 Orlando: Academic Press Inc., p 43-105.
- 13 Nézan E, Tillmann U, Bilien G, Boulben S, Chèze K, Zentz F, et al. 2012. Taxonomic revision
14 of the dinoflagellate *Amphidoma caudata*: transfer to the genus *Azadinium*
15 (Dinophyceae) and proposal of two varieties, based on morphological and molecular
16 phylogenetic analyses. *Journal of Phycology* 48:925-39.
- 17 Ofuji K, Satake M, McMahon T, Silke J, James KJ, Naoki H, et al. 1999. Two analogs of
18 Azaspiracid isolated from mussels, *Mytilus edulis*, involved in human intoxication in
19 Ireland. *Natural Toxins* 7:99-102.
- 20 Pedersen MF, Hansen PJ. 2003. Effects of high pH on the growth and survival of six marine
21 heterotrophic protists. *Marine Ecology Progress Series* 260:33-41.
- 22 Percopo I, Siano R, Rossi R, Soprano V, Sarno D, Zingone A. 2013. A new potentially toxic
23 *Azadinium* species (Dinophyceae) from the Mediterranean Sea, *A. dexteroporum* sp.
24 nov. *Journal of Phycology* 5: 950-66.
- 25 Pfiester LA, Anderson DM. 1987. Dinoflagellate reproduction. In: Taylor FJR, editor. *The*
26 *Biology of Dinoflagellates*. New York: Academic Press, p 611-48.
- 27 Potvin E, Hwang YJ, Yoo YD, Kim JS, Jeong HJ. 2013. Feeding by heterotrophic protists and
28 copepods on the photosynthetic dinoflagellate *Azadinium* cf. *poporum* from Western
29 Korean waters. *Aquatic Microbial Ecology* 68: 143-58.
- 30 Rampi L. 1969. Su alcuni elementi fitoplanctonici (Peridinee, Silicococcales ed
31 Heterococcales) rari o nuovi raccolti nelle acque del Mare Ligure. *Natura* (Milano)
32 60:49-56.
- 33 Rost B, Richter KU, Riebesell U, Hansen PJ. 2006. Inorganic carbon acquisition in red tide
34 dinoflagellates. *Plant, Cell and Environment* 29:810-22.

- 1 Salas R, Tillmann U, John U, Kilcoyne J, Burson A, Cantwell C, et al. 2011. The role of
2 *Azadinium spinosum* (Dinophyceae) in the production of Azaspiracid Shellfish
3 Poisoning in mussels. *Harmful Algae* 10:774-83.
- 4 Satake M, Ofuji K, James K, Furey A, Yasumoto T. 1998. New toxic events caused by Irish
5 mussels. In: Reguera B, Blanco J, Fernandez ML, Wyatt T, editors. *Harmful Algae*.
6 Santiago de Compostela: Xunta de Galicia and International Oceanographic
7 Commission of UNESCO, p 468-9.
- 8 Schmidt LE, Hansen PJ. 2001. Allelopathy in the prymnesiophyte *Chrysochromulina*
9 *polylepis*: effect of cell concentration, growth phase and pH. *Marine Ecology Progress*
10 *Series* 216:67-81.
- 11 Schnepf E, Elbrächter M. 1999. Dinophyte chloroplasts and phylogeny - A review. *Grana*
12 38:81-97.
- 13 Silva ES. 1968. Plancton da lagoa de Óbidos (III). Abundância, variações sazonais e grandes
14 "blooms". *Notas e estudos di Instituto de Biologia Marítima* 34:1-79, 7 pl.
- 15 Smayda TJ. 1997. Harmful algal blooms: Their ecophysiology and general relevance to
16 phytoplankton blooms in the sea. *Limnology and Oceanography* 42:1137-53.
- 17 Smayda TJ. 2002a. Turbulence, watermass stratification and harmful algal blooms: an
18 alternative view and frontal zones as "pelagic seed banks". *Harmful Algae* 1:95-112.
- 19 Smayda TJ. 2002b. Adaptive ecology, growth strategies and the global bloom expansion of
20 dinoflagellates. *Journal of Oceanography* 58:281-94.
- 21 Soederberg LM, Hansen PJ. 2007. Growth limitation due to high pH and low inorganic carbon
22 concentrations in temperate species of the dinoflagellate genus *Ceratium*. *Marine*
23 *Ecology Progress Series* 351:103-12.
- 24 Sohn MH, Seo KW, Choi YS, Lee SJ, Kang YS, Kang YS. 2011. Determination of the
25 swimming trajectory and speed of chain-forming dinoflagellate *Cochlodinium*
26 *polykrikoides* with digital holographic particle tracking velocimetry. *Marine Biology*
27 158:561-70.
- 28 Taleb H, Vale P, Amanhir R, Benhadouch A, Sagou R, Chafik A. 2006. First detection of
29 azaspirazids in mussels in north west Africa. *Journal of Shellfish Research* 25:1067-
30 70.
- 31 Taylor BB, Torrecilla E, Bernhardt A, Taylor MH, Peeken I, Röttgers R, et al. 2011. Bio-
32 optical provinces in the eastern Atlantic Ocean and their biogeographical relevance.
33 *Biogeosciences* 8:3609-29.
- 34 Tillmann U. 2004. Interactions between planktonic microalgae and protozoan grazers. *Journal*

1 of Eukaryotic Microbiology 51:156-68.

2 Tillmann U, Elbrächter M, Krock B, John U, Cembella A. 2009. *Azadinium spinosum* gen. et
3 sp. nov. (Dinophyceae) identified as a primary producer of azaspiracid toxins.
4 European Journal of Phycology 44:63-79.

5 Tillmann U, Elbrächter M. 2010. Plate overlap pattern of *Azadinium spinosum* Elbrächter et
6 Tillmann (Dinophyceae), the newly discovered primary source of azaspiracid toxins.
7 In: Ho KC, Zhou MJ, Qi YZ, editors. Proceedings of the 13th International
8 Conference on Harmful Algae. Hong Kong: Environmental Publication house, p 42-4.

9 Tillmann U, Elbrächter M, John U, Krock B, Cembella A. 2010. *Azadinium obesum*
10 (Dinophyceae), a new nontoxic species in the genus that can produce azaspiracid
11 toxins. Phycologia 49:169-82.

12 Tillmann U, Elbrächter M, John U, Krock B. 2011. A new non-toxic species in the
13 dinoflagellate genus *Azadinium*: *A. poporum* sp. nov. European Journal of Phycology
14 46:74-87.

15 Tillmann U, Salas R, Gottschling M, Krock B, O'Driscoll D, Elbrächter M. 2012a.
16 *Amphidoma languida* sp. nov. (Dinophyceae) reveals a close relationship between
17 *Amphidoma* and *Azadinium*. Protist 163:701-19.

18 Tillmann U, Soehner S, Nézan E, Krock B. 2012b. First record of *Azadinium* from the
19 Shetland Islands including the description of *A. polongum* sp. nov. Harmful Algae
20 20:142-55.

21 Tillmann U, Elbrächter M. 2013. Mode of cell division in *Azadinium spinosum*. Botanica
22 Marina 56: 399-408

23 Tomas RN. 1974. Cell division in *Gonyaulax catenella*, a marine catenate dinoflagellate.
24 Journal of Protozoology 21:316-21.

25 Totti, C., Civitarese, G., Acri, F., Barletta, D., Candelari, G., Paschini, E. Solazzi, A. 2000.
26 Seasonal variability of phytoplankton populations in the middle Adriatic sub-basin. J.
27 Plankton Res. 22:1735–56.

28 Ueoka R, Ito A, Izumikawa M, Maeda S, Takagi M, Shin-Ya K, et al. 2009. Isolation of
29 azaspiracid-2 from a marine sponge *Echinoclathria* sp as a potent cytotoxin. Toxicon
30 53:680-84.

31 Viličić, D., Leder, N., Gržetić, Z. & Jasprica, N. 1995. Microphytoplankton in the Strait of
32 Otranto (eastern Mediterranean). Marine Biology 123:619–30.

33 Yao J, Tan Z, Zhou D, Guo M, Xing L, Yang S. 2010. Determination of azaspiracid-1 in
34 shellfishes by liquid chromatography with tandem mass spectrometry. Chinese Journal

1 of Chromatography 28:363–7.
2 Zapata M, Frage S, Rodriguez F, Garrido JL. 2012. Pigment-based chloroplast types in
3 dinoflagellates. Marine Ecology Progress Series 465:33-52.
4 Zhu M, Tillmann U. 2012. Nutrient starvation effects on the allelochemical potency of
5 *Alexandrium tamarense* (Dinophyceae). Marine Biology 159:1449-59.

6
7
8

1 Tab. 1: *Azadinium caudatum* var. *margalefii*, swimming speed, summary statistics of
 2 swimming paths depicted in Fig. 2.
 3

Track no	Distance – duration	Speed ($\mu\text{m s}^{-1}$) (mean \pm Std)	Speed ($\mu\text{m s}^{-1}$) (min – max)
1	121 μm – 2.80 s	43 \pm 6	31 – 52
2	297 μm – 4.24 s	81 \pm 67	36 – 363
3	200 μm – 1.60 s	138 \pm 6	130 – 145
4	162 μm – 2.68 s	116 \pm 122	21 – 389
5	118 μm – 1.23 s	88 \pm 12	69 – 118
6	412 μm – 6.00 s	69 \pm 38	31 – 223
7	135 μm – 1.60 s	84 \pm 11	67 – 99
8	120 μm – 2.40 s	50 \pm 7	36 – 57
9	145 μm – 2.36 s	61 \pm 6	52 – 75
10	47 μm – 1.00 s	47 \pm 5	31 – 52
11	87 μm – 1.12 s	135 \pm 104	31 – 363
12	96 μm – 1.24 s	114 \pm 81	39 – 234
13	287 μm – 5.00 s	57 \pm 5	52 – 70
14	314 μm – 5.60 s	56 \pm 5	47 – 67
15	370 μm – 5.00 s	74 \pm 37	47 – 197
16	69 μm – 1.20 s	57 \pm 16	44 – 78
17	212 μm – 1.60 s	184 \pm 67	47 – 260
18	112 μm – 1.16 s	135 \pm 72	65 – 234
19	148 μm – 2.20 s	67 \pm 11	52 – 88
20	64 μm – 1.40 s	46 \pm 6	36 – 52
21	101 μm – 1.20 s	84 \pm 7	75 – 93
22	51 μm – 0.80 s	64 \pm 20	47 – 83
23	145 μm – 2.72 s	65 \pm 39	42 – 183
24	143 μm – 1.72 s	83 \pm 67	26 – 260
25	73 μm – 0.56 s	131 \pm 72	65 – 337
26	153 μm – 2.60 s	59 \pm 7	42 – 67
27	246 μm – 5.60 s	44 \pm 5	34 – 60
28	170 μm – 1.40 s	121 \pm 60	65 – 285
29	109 μm – 1.16 s	94 \pm 58	39 – 247
30	149 μm – 1.36 s	110 \pm 88	26 – 234

4
 5

1 Tab. 2: Pigment composition of *Azadinium caudatum* var. *margalefii* AC1 in percent of total
2 pigment, mean \pm standard deviation (SD)

Pigment	[%] of total pigment
Chlorophyll a	42.3 \pm 0.8
Perididin	38.3 \pm 0.9
Chlorophyll c ₁ +c ₂	10.0 \pm 2.2
Diadinoxanthin	6.0 \pm 0.6
Dinoxanthin	2.0 \pm 0.2
β , β -carotene	1.1 \pm 0.04
Diatoxanthin	0.2 \pm 0.01
Violaxanthin	0.1 \pm 0.01

3
4
5
6
7

1 Figure legends

2

3 **Fig. 1:** *Azadinium caudatum* var. *margalefii*, LM of live (B, C) and fixed cells (all other). A-E:

4 General size and shape. F: Cells stained with DAPI and viewed with UV excitation in

5 normal light to show the shape and location of the nucleus. G-H; epifluorescence view

6 (UV excitation) of two different DAPI stained cells, note the enlarged and elongated

7 nucleus in H. I-J: Two different cells fixed with a mixture of formalin and Lugol, note

8 the presence of large and brownish stained vesicles of probable reserve material. K-O:

9 Epifluorescence view of formalin fixed cells; chlorophyll autofluorescence to show

10 chloroplast structure. N and O represent two different focal planes of the same cell in

11 posterior view. Note the sulcal area void of chloroplast extensions (white arrow). Scale

12 bars = 10 μ m.

13 **Fig. 2:** Swimming paths of *Azadinium caudatum* var. *margalefii*. Time interval between each

14 small white dot is 0.04 s, between each large dot is 0.2 s, and between each black dot 1

15 s. Swimming direction indicated by the orientation of the cells (not drawn to scale).

16 Numbers in circles refer to Tab. 1, where summary statistics for each path are listed.

17 **Fig. 3:** SEM micrographs of thecae of different cells. A: Whole cell in lateral view. B: Internal

18 view of the hypotheca and the sulcal area. C-D: Detailed internal (C) and external (D)

19 view of the anterior sulcal plate showing that plate Sa is overlapped by plate C1 (white

20 arrows) and is overlapping plate C6 (black arrows). Scale bars = 5 μ m (A, B) or 2 μ m

21 (C, D).

22 **Fig. 4:** Cell division of *Azadinium caudatum* var. *margalefii*. LM (A-L), SEM (M-P), or

23 schematic drawing (Q-R). A-B: Cells fixed with formalin/lugol, different stages of cell

24 division. C-D, E-F, G-H, I-J, and K-L: Pairs of the same cell stained with calcofluor

25 white in bright field (left) or with UV excitation (right). C-H: different stages of cell

26 division. I-L: freshly divided cells showing that half of the plates are still missing. M-P:

1 SEM of different cells. M: Ventral/lateral view of a cell presumably close to cell
2 division. N-P: Cells in cell division, in ventral (N), dorsal (O), or antapical (P) view. Q-
3 R: Schematic view of fission line of epitheca (Q) and hypotheca (R) separating the
4 anteriosinistral daughter cell (light shaded) and the posteriodextral daughter cell (darker
5 shaded). Arrowheads indicate direction of plate overlap at the fission line with black
6 symbols indicating plate margins overlapping the plate with the corresponding white
7 symbols. Plate overlap adapted from Nézan et al. (2012). Plate labels according to the
8 Kofoidean system: apical plates: 1' - 4' (surrounding the apical pore complex);
9 intercalary plates: 1 a, 2 a, 3a; precingular plates: 1'' - 6''; postcinguar plates: 1''' -
10 6'''; antapical plates: 1'''' , 2''''; Sa = anterior sulcal plate; Sp = posterior sulcal plate.
11 Scale bars = 10 μm

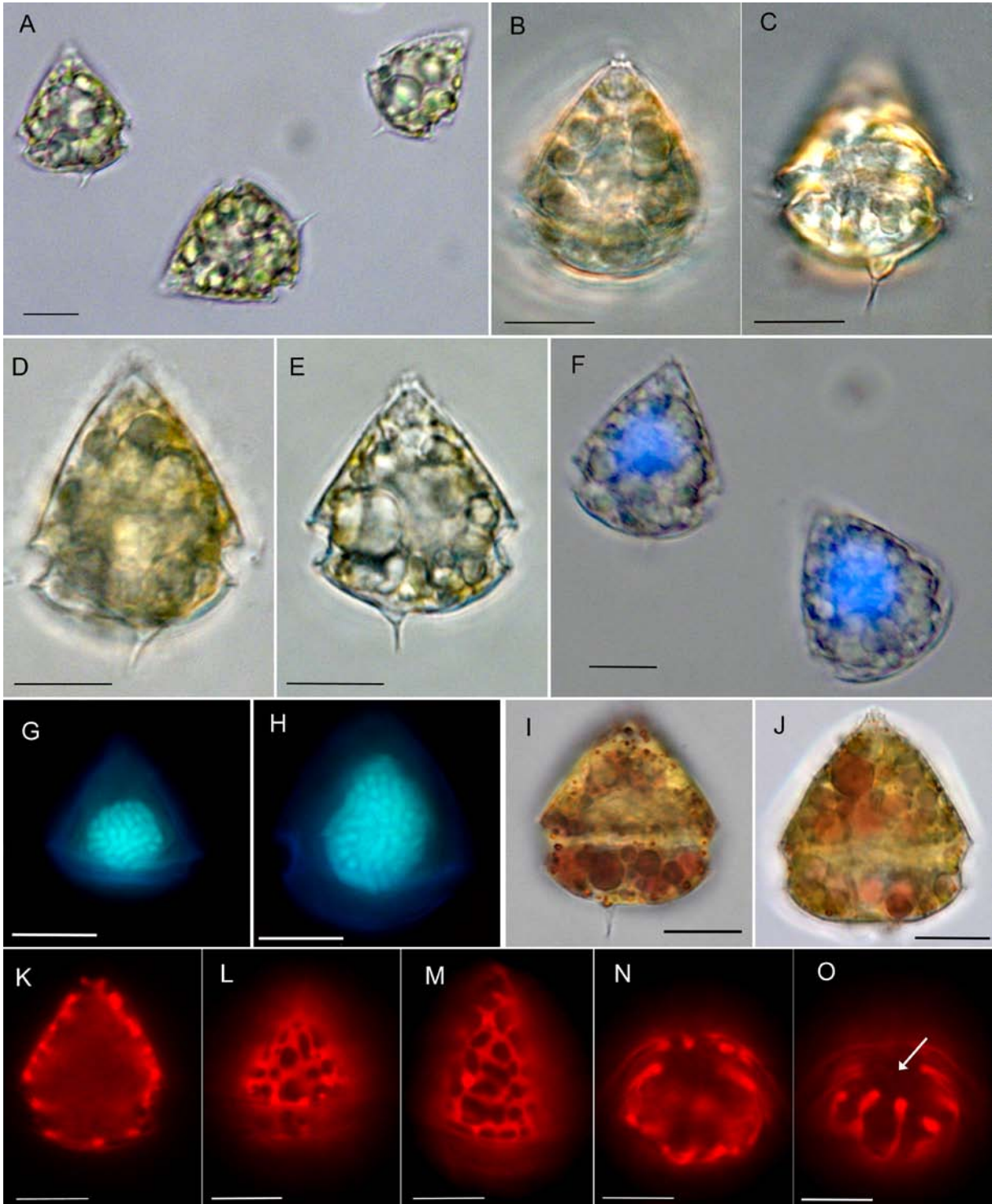
12 **Fig. 5:** Growth performance of *Azadinium caudatum* var. *margalefii* in response to
13 temperature and irradiance. A-F: Cell concentration (log scale) versus day after
14 inoculation at different temperatures (right) or different irradiances (left). Black dots:
15 data used to calculate growth rate. Arrows: results of pH measurements on day 21. G:
16 growth rate μ (d^{-1}) (black dots) as a function of irradiance. The dotted line represents a
17 Michaelis-Menten curve fit. H: Growth rate μ (d^{-1}) for three different temperatures.
18 Note that growth at 15° C and 100 $\mu\text{E m}^{-2} \text{s}^{-1}$ (D) was used for both analyses. Data
19 points or bars represent treatment mean \pm 1SD (n = 3).

20 **Fig. 6:** High-performance liquid chromatography chromatogram of photosynthetic pigments
21 (detection at 434 nm) of *Azadinium caudatum* var. *margalefii* AC1. Retention time on
22 the x-axis; absorbance (AU: arbitrary units) on the y-axis.

23 **Fig. 7:** Absorption spectra of four unknown pigments.

24

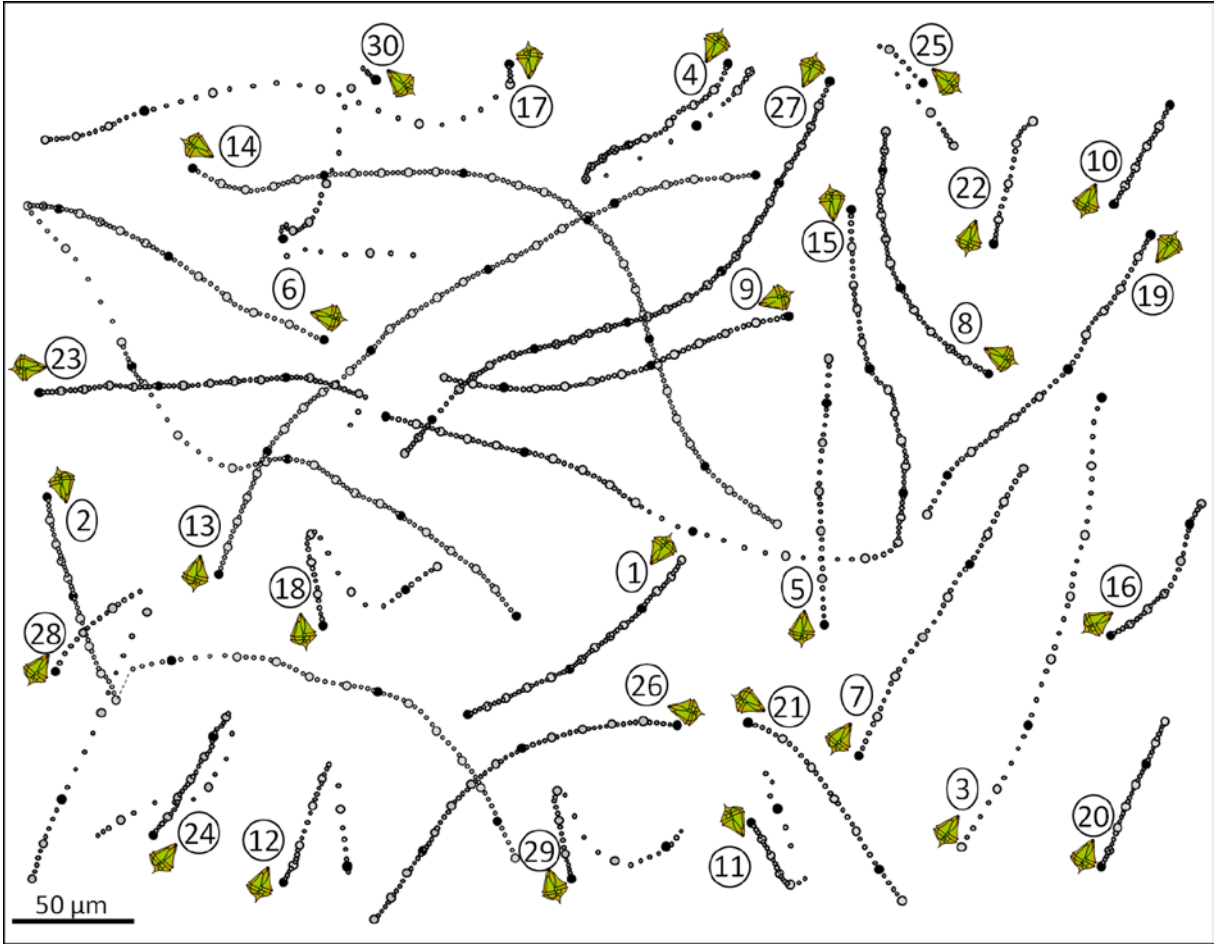
1



2
3
4
5

Fig. 1

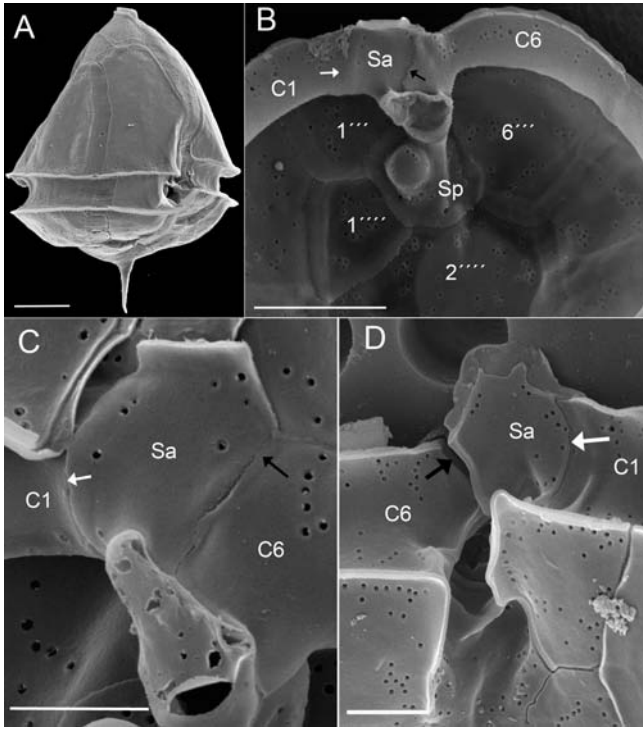
1



2
3
4
5

Fig. 2

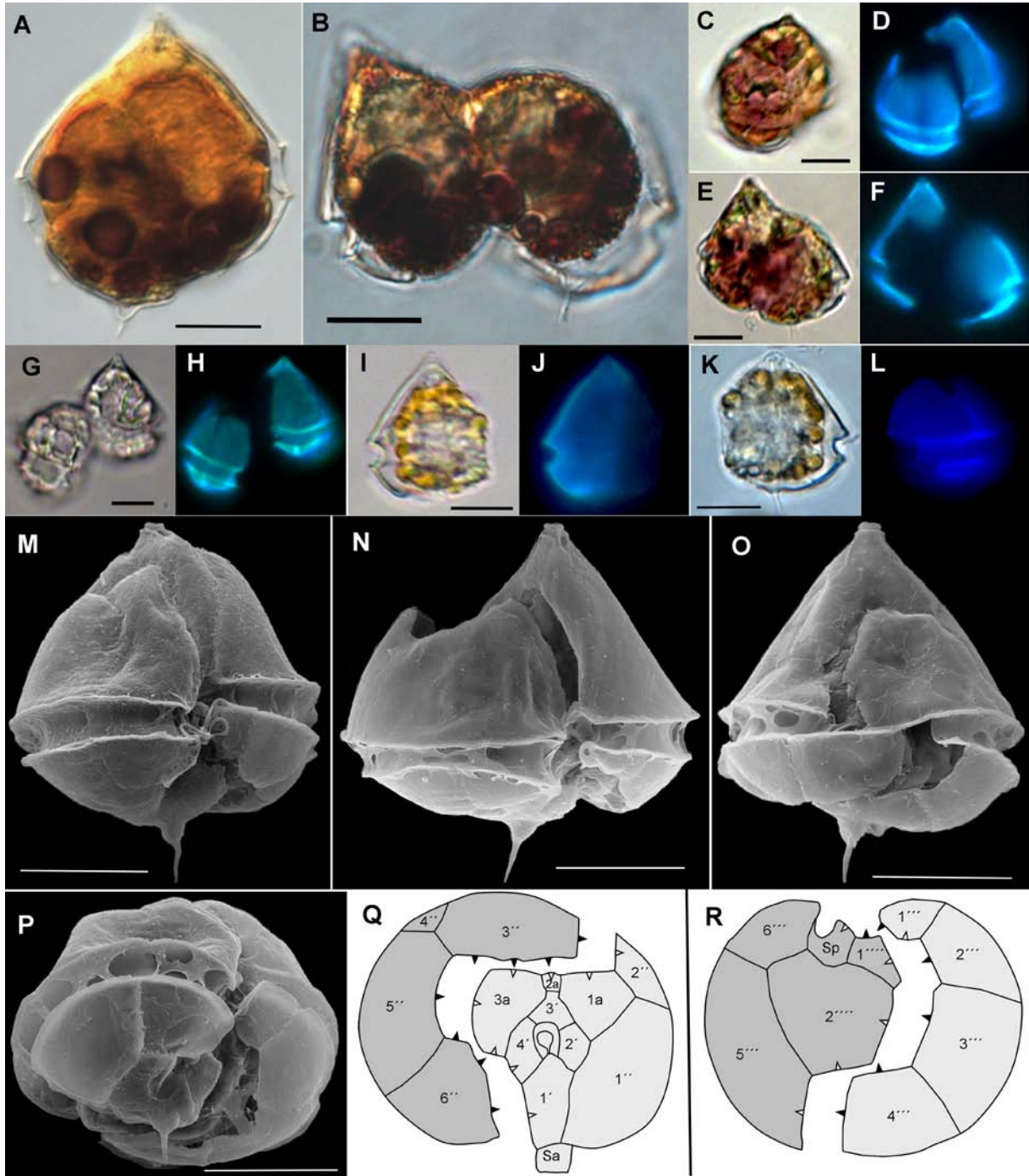
1



2
3
4
5

Fig. 3

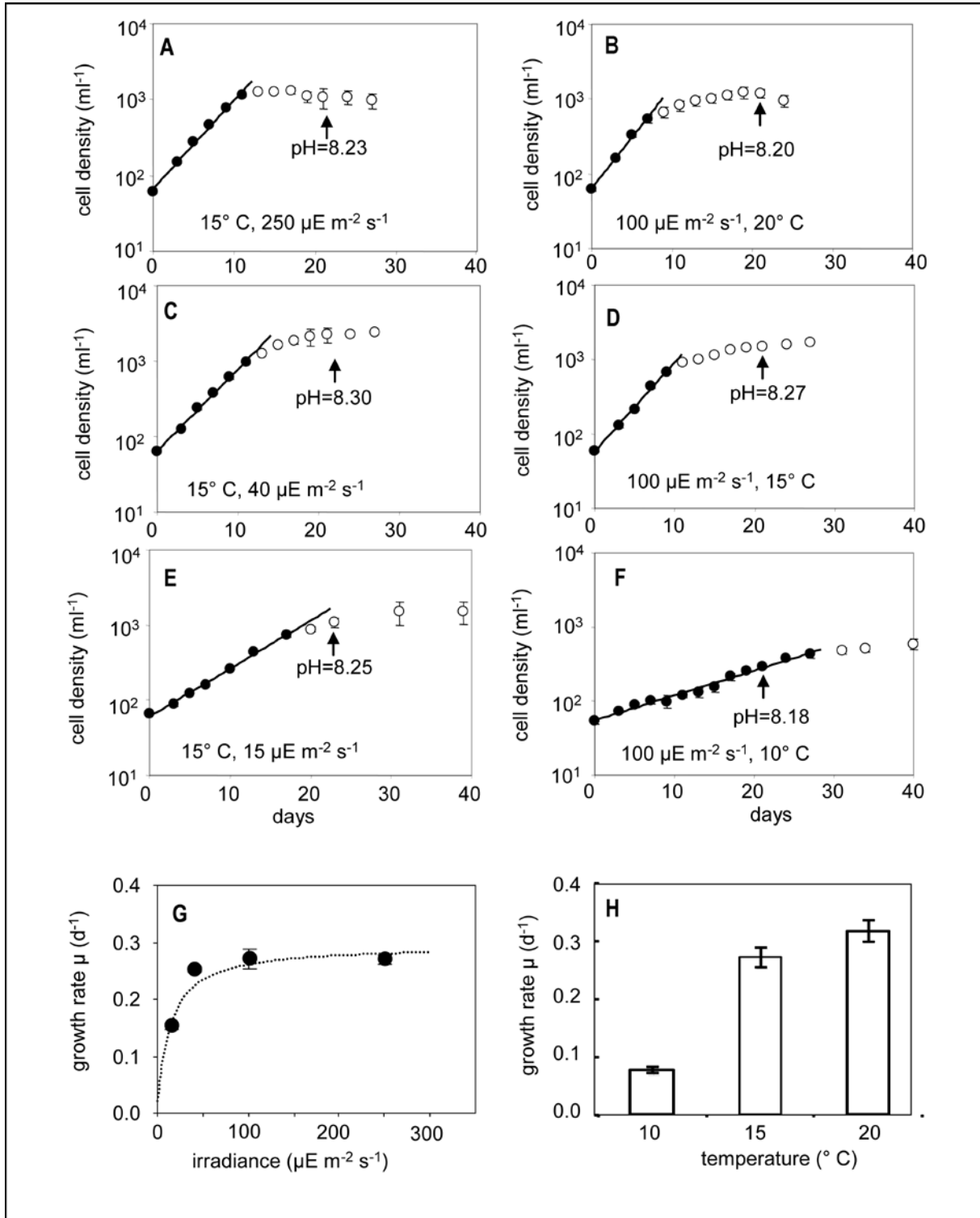
1



2
3
4
5

Fig. 4

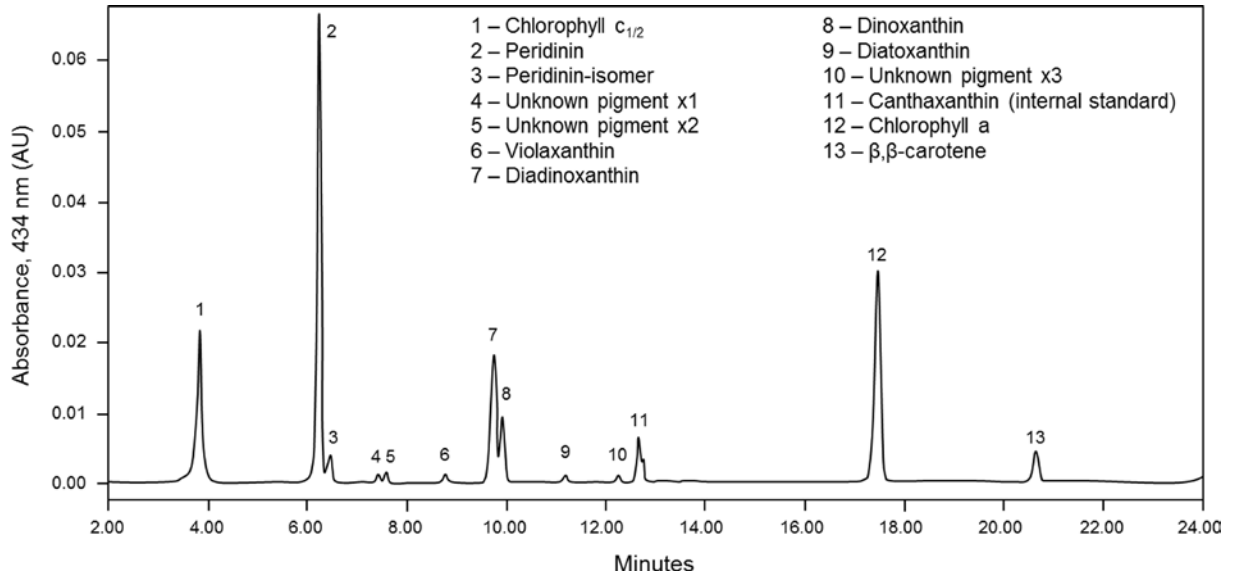
1



2
3
4
5

Fig. 5

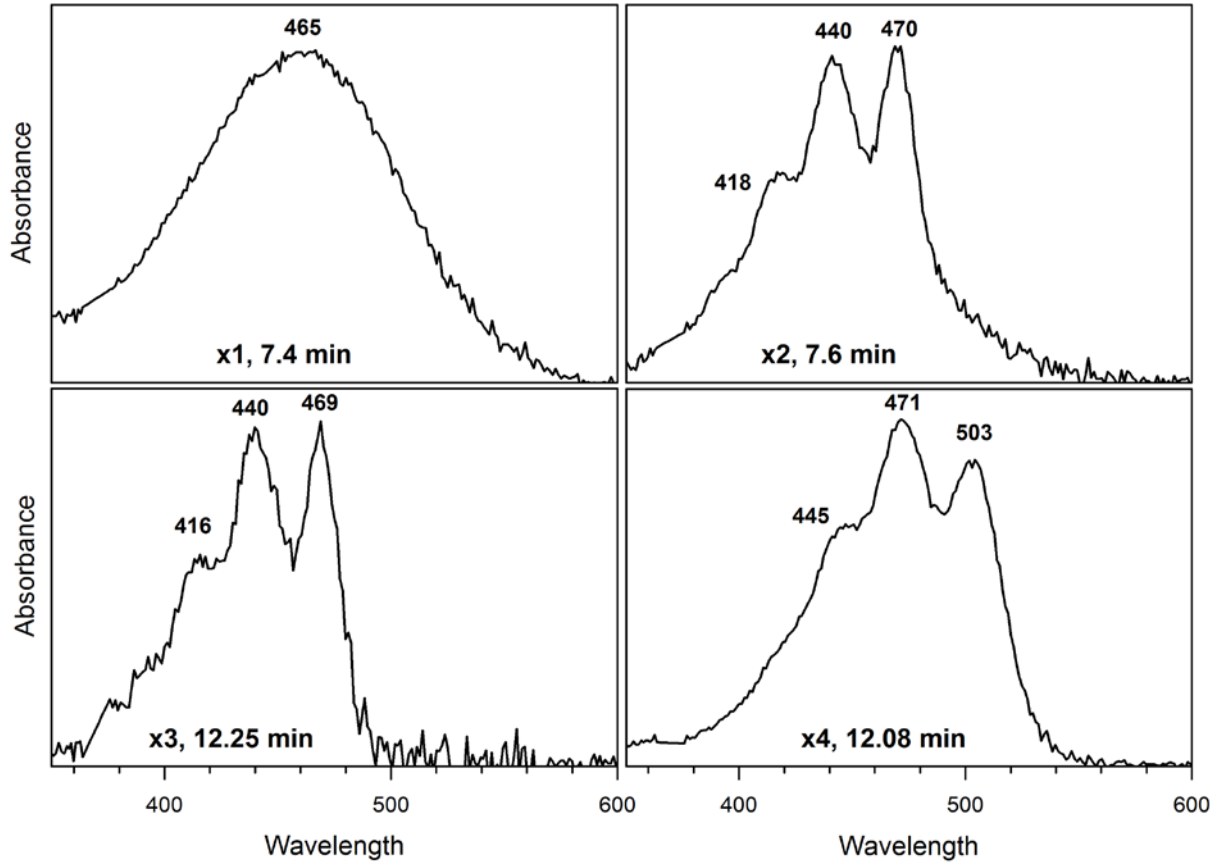
1



2
3
4
5

Fig. 6

1



2
3
4

Fig. 7